

## Modeling the Response of an Idealized Coastal Ocean to a Traveling Storm and to Flow over Bottom Topography

LEIV H. SLØRDAL,\* EIVIND A. MARTINSEN,<sup>†</sup> AND ALAN F. BLUMBERG\*\*

\* *Institute of Geophysics, University of Oslo, Oslo, Norway*

<sup>†</sup> *The Norwegian Meteorological Institute, Oslo, Norway*

\*\* *HydroQual, Inc., Mahwah, New Jersey*

(Manuscript received 14 August 1992, in final form 2 June 1993)

### ABSTRACT

To validate a three-dimensional hydrodynamic model for use in coastal waters, two test cases with idealized geometry and forcing functions were performed. The tests involve the barotropic and baroclinic response of a coastal ocean with a uniform alongshore shelf to the passage of a storm and the circulation induced by flow over a topographic feature. The model used in this study is the estuarine, coastal, and ocean model developed by Blumberg and Mellor. The model is three dimensional and solves for three components of the current field, temperature, and salinity. The model has a terrain-following sigma ( $\sigma$ ) coordinate system, a coastal-following curvilinear grid in the horizontal, and an embedded second-order turbulence closure submodel to provide vertical mixing coefficients and uses the free surface as a prognostic variable. At the open boundaries, a flow relaxation scheme (FRS) has been implemented to pass out internally generated disturbances with minimum reflection. The results from the first test case demonstrate that the model successfully reproduces the expected theoretical response to a traveling storm. Both standing and propagating shelf waves with the proper spatial structure are found. In the upper part of the ocean, wind-generated oscillations are the dominant response. In the second test case, a stationary anticyclone forms over the topographic feature and a cyclonic eddy is shed downstream in a time of the order of the advective timescale, in agreement with theory and previous studies. When investigating the long-term evolution, the model simulations reproduce the baroclinic instability mechanisms expected from analytical considerations.

### 1. Introduction

In recent years, the waters along the coast of Norway have been the subject of many observational and theoretical studies. Much of the motivation for these studies has been the extension of oil and gas drilling and production activities onto the Norwegian continental shelf. These activities in the Norwegian Coastal Current (NCC) clearly provide a range of challenges for the offshore industry's exploration and production personnel. To meet these challenges, the Operators' Committee North (OKN) initiated a MetOcean Modeling Project (MOMOP), with the goal of developing a three-dimensional hydrodynamic model to forecast and hindcast the Norwegian coastal waters. In the first phase, OKN subjected several models to idealized test cases. In the second phase, two of these models were selected for further tests to ensure that they contained the basic physics of the processes relevant to Norwegian coastal waters. This paper describes the results from one of the selected models. This numerical model is now operational at the Norwegian Meteorological In-

stitute, where forecasts of the Norwegian Coastal Current System are being routinely produced.

The NCC consists of relatively fresh water from the Baltic Sea, the Skagerrak, and fjords and rivers along the Norwegian coast. The wedge-shaped NCC is surrounded by the more saline Atlantic water, which enters this area mainly through the Faroe-Shetland Channel. A typical  $\sigma_t$  value of the Atlantic water is 27.5;  $\sigma_t$  values of the surface water of the NCC will typically vary between 22.0 and 26.0 depending on the season. The bottom topography along the western coast of Norway is characterized by a continental shelf with an average width of 200 km and an average depth of 300 m. There are large depth variations on the shelf due to numerous deep trenches and shallow bank areas. Measurements (Eide 1979) and numerical experiments (Ikeda et al. 1989) indicate that several of these banks seem to be important factors for eddy and meander formation in the NCC. The continental slope is rather steep and leads down to the deep ocean of the Norwegian Sea with typical depths of 3000 m. The large-scale dynamics of this area is strongly influenced by storm-induced topographic shelf waves, giving surge and current oscillations with a period of approximately one day (Martinsen et al. 1979; Gordon and Huthnance 1987; Gjevik 1991). There is also evidence of strong current

---

Corresponding author address: Dr. Leiv H. Slørdal, Institute of Geophysics, University of Oslo, P.O. Box 1022 Blindern, Oslo, N-0315, Norway.

oscillations with near inertial period, as a consequence of storm forcing (Gjevik 1991).

Two test cases were conducted to investigate how well, at least in a qualitative sense, the numerical model could handle the aforementioned types of dynamic processes, which are of major importance in the NCC. The first of these processes is the large-scale dynamic shelf response, set up by a storm passage. The second process is concerned with the generation of meanders and eddies induced by flow over a topographic feature. Detailed description of each of the two test cases, and results from model simulations of each, are provided in section 3. Based on the material presented, other investigators should be able to perform the same experiments for their own model validation purposes.

## 2. Description of the model

The model used in this study is the time-dependent, three-dimensional, estuarine and coastal circulation model of Blumberg and Mellor (see Blumberg and Mellor 1983, 1987). This model has been used successfully in numerous studies on various important natural water systems; among them are works by Blumberg and Mellor (1983) on the South Atlantic Bight, Mellor and Ezer (1991) on the Gulf Stream region, Blumberg and Galperin (1990) on the New York Bight, and Blumberg and Goodrich (1990) on Chesapeake Bay.

This model is a three-dimensional, primitive equation, time-dependent estuarine, coastal, and open-ocean circulation model. The prognostic variables are the free surface elevation, the three components of velocity, temperature, salinity (hence, density through an equation of state), and two quantities that characterize the turbulence: turbulent kinetic energy and turbulent macroscale. Free surface elevation is calculated prognostically with only some sacrifice in computational time so that tides and storm surge events can also be simulated. This is accomplished by use of a mode-splitting technique whereby the volume transport and vertical velocity shear are solved separately. The vertical mixing processes are calculated by applying an analytical turbulence closure model of small-scale turbulence (Mellor and Yamada 1982; Galperin et al. 1988). A sigma ( $\sigma$ ) coordinate system, such that the number of grid points in the vertical is independent of depth, is incorporated in the model. Another transformation, this one to an orthogonal curvilinear coordinate system for the horizontal coordinates, permits considerable latitude in the design of a computational grid network. The model responds to forcing from surface wind stress, atmospheric pressure gradients, heat flux, salinity flux, tidal forcing, freshwater discharge, and other lateral boundary conditions imposed by the region outside of the domain of interest.

At the open boundaries, the flow relaxation scheme (FRS) of Martinsen and Engedahl (1987) has been

implemented for both of the test cases presented here. This scheme was originally designed to relax external solutions derived from a large area model toward solutions in a limited-area model with a finer grid resolution. The relaxation takes place within specified zones (FRS zones) applied at the open boundaries. In the FRS zones, the variables are redefined or relaxed by the following equation:

$$\phi = \alpha\phi_{\text{ext}} + (1 - \alpha)\phi_{\text{int}}, \quad (1)$$

where  $\phi_{\text{ext}}$  is the prescribed external solution,  $\phi_{\text{int}}$  is the calculated interior solution, and  $\phi$  is the new updated value in the FRS zone. The relaxation parameter  $\alpha$  varies between 0 and 1 within the relaxation zones. It is equal to 1 at the outer ends of the zones and decreases smoothly toward 0 at the inner ends. When the external solution is set to a constant, the FRS method degenerates to a sponge-type open boundary condition.

The equations of the hydrodynamic model, together with their boundary conditions, are solved by finite-difference techniques. The computational grid arrangement of points is based on the "C" stencil. The time differencing is leapfrog and an implicit numerical scheme in the vertical direction has been adopted for computational efficiency. At every time step, the solution is filtered to remove any residual time splitting (Asselin 1972). For advection, a variant of the Lilly (1965) scheme is used. The Holland and Lin (1975) scheme is used for the Coriolis force. Horizontal friction is lagged in time for computational stability. The numerical scheme conserves mass and total energy except for the time filter and explicit sources and sinks due to friction.

## 3. Case I: Storm-induced motions

The response of a coastal ocean to a traveling storm is a problem of much interest. It is well known that a significant part of the transient currents and surface elevation in the coastal ocean is due to shelf waves. Topographic shelf waves have been studied extensively by Mysak (1980) and Huthnance et al. (1986). Using a numerical barotropic model, Martinsen et al. (1979) examined the importance of these kinds of waves in connection with storm surge events along the western coast of Norway. Recently, Gjevik (1991) has studied the large-scale response of a low pressure center moving across a straight shelf-slope area through the use of a layered (baroclinic) numerical ocean model.

Since the response to traveling storms is so important in this area, a slightly modified version of the experiment described by Gjevik (1991) was performed. The main reason for doing this was to examine how well the model responded to this simple, but realistic, atmospheric forcing.

The model domain, the idealized topography, and initial density distribution for this test case are shown in Figs. 1 and 2. The initial position and the track of

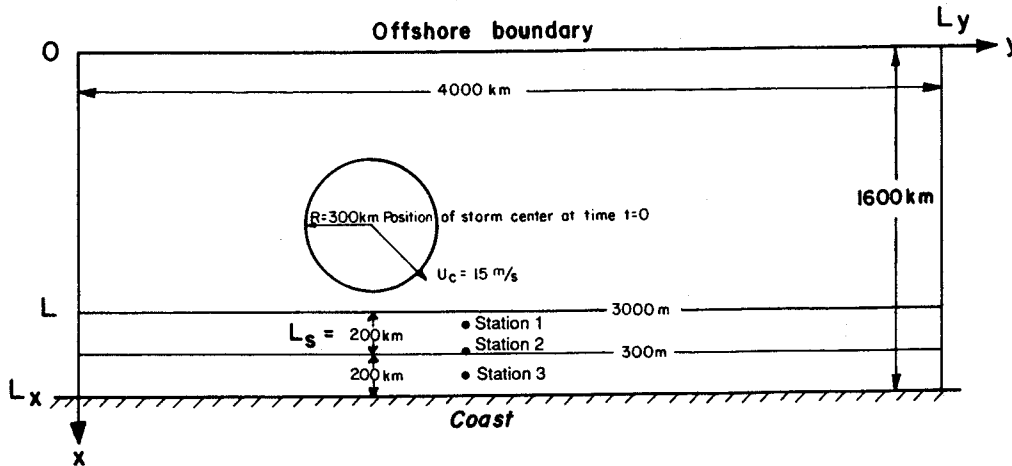


FIG. 1. Sketch of the model domain for test case 1. Position and horizontal length scale of storm center as well as positions of time series locations are noted.

the low pressure center are also shown in Fig. 1; in addition, stations where time series have been computed are marked. The topography is given as a straight coast along  $x = L_x$ ; a straight shelf of depth  $H_S$  and width of  $L_S$ ; a linear slope of the same width,  $L_S$ ; and a deep ocean with depth  $H$  and width of  $L = L_x - 2L_S$ . In this experiment  $H = 3000$  m,  $H_S = 300$  m,  $L_x = 1600$  km,  $L_S = 200$  km, and  $L = 1200$  km. The alongshore extent of the domain is  $L_y = 4000$  km. The FRS is used at the open boundaries:  $x = 0$ ,  $y = 0$ , and  $y = L_y$ . The stratification consists of an upper layer with constant density  $\rho_0$  and thickness  $h_1$ , a middle layer with density increasing linearly from  $\rho_0$  to  $\rho_b$  and thickness  $h_2 - h_1$ , and a lower layer with constant density  $\rho_b$  and thickness  $H - h_2$ . Here  $\rho_0 = 1026.0$  kg m<sup>-3</sup>,  $\rho_b = 1027.5$  kg m<sup>-3</sup>,  $h_1 = 50$  m, and  $h_2 = 500$  m (Fig. 2). A grid size of 20 km was employed in both hori-

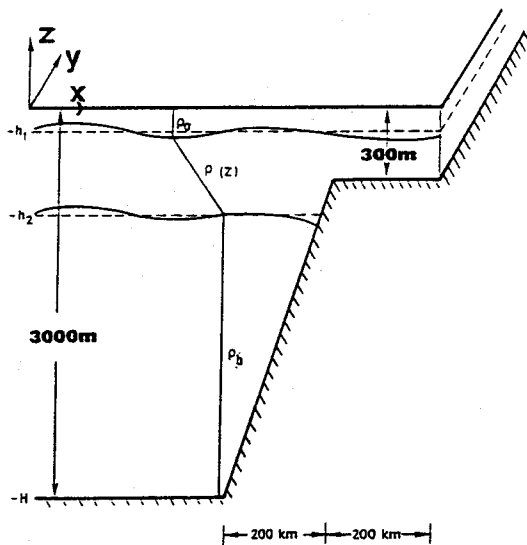


FIG. 2. Cross section of the model domain for test case 1.

zontal directions. The grid consisted of  $80 \times 200$  points. In the vertical, 10  $\sigma$  levels were used. A time step of 36 s was used for the external mode, while the internal mode was solved with a time step of 900 s. The total simulation time for this test case was 72 hours.

The atmospheric pressure distribution for the traveling cyclone is given by

$$P_A(r, t) = P_M - P_c(t)e^{-(r/R)^2}, \quad (2)$$

where  $P_A$  is the pressure,  $P_M$  is the mean pressure,  $P_c$  is the pressure perturbation of the cyclone center,  $r$  is the distance from the center, and  $R$  is a horizontal length scale for the cyclone. In this test case,  $R = 300$  km and  $r$  is given by

$$r = [(x - x_c(t))^2 + (y - y_c(t))^2]^{1/2}, \quad (3)$$

where  $x_c$  and  $y_c$  are the coordinates of the moving cyclone center. Relative to the coordinate frame given in Fig. 1, the initial position of the cyclone is  $x_c(0) = 800$  km and  $y_c(0) = 1340$  km. The center is moving with a speed  $u_c = 15$  m s<sup>-1</sup> toward the shore, at an angle of 45 degrees with the coast. The time dependence of the pressure perturbation is given by

$$P_c(t) = \begin{cases} P_0 t / t_s, & 0 \leq t \leq t_s \\ P_0, & t_s < t \leq t_D - t_s \\ P_0(t_D - t) / t_s, & t_D - t_s < t \leq t_D \\ 0, & t_D < t, \end{cases} \quad (4)$$

where  $P_0 = 40$  hPa,  $t_s = 12$  h, and  $t_D = 30$  h. The wind speed is calculated by the following gradient wind formula (Hess 1959):

$$W(r) = \left[ \frac{r}{\rho_A} \frac{\partial P_A}{\partial r} + \left( \frac{rf}{2} \right)^2 \right]^{1/2} - \frac{rf}{2}, \quad (5)$$

where  $f = 1.3 \times 10^{-4}$  s<sup>-1</sup> is the Coriolis parameter and  $\rho_A = 1.3$  kg m<sup>-3</sup> is the density of the air. The shear

stress,  $\tau_s(r)$ , is in the direction of the wind and has the magnitude of

$$\tau_s(r) = \rho_A C_d^W W^2(r), \quad (6)$$

where  $C_d^W$  is the drag coefficient given by (Large and Pond 1981)

$$C_d^W = 0.7 \times 10^{-3} \begin{cases} 1.2, & W \leq 11 \text{ m s}^{-1} \\ 0.49 + 0.065 W, & W > 11 \text{ m s}^{-1}. \end{cases} \quad (7)$$

With the given values of the physical constants, a maximum wind speed of  $32.8 \text{ m s}^{-1}$ , giving a maximum surface stress of  $2.56 \text{ Pa}$ , is found at a distance of  $0.85R$  ( $=255 \text{ km}$ ) from the cyclone center. At a distance of  $2R$  ( $=600 \text{ km}$ ) the wind speed is reduced to  $5.4 \text{ m s}^{-1}$  and the stress is only  $0.032 \text{ Pa}$ . The shear stress at the bottom is given by the following nonlinear condition:

$$A_v \left( \frac{\partial u}{\partial z}, \frac{\partial v}{\partial z} \right) = C_D (u^2 + v^2)^{1/2} (u, v);$$

$$z = -H(x, y), \quad (8)$$

where  $A_v$  is the vertical eddy diffusion coefficient and  $C_D$  is the bottom drag coefficient. A value of  $0.0025$  is used for  $C_D$ .

### Results/discussion

In Fig. 3 the temporal evolution of the sea surface elevation is shown; only a subregion of the total computational domain is given. The lower axis yields the alongshore position and the right axis measures the distance offshore. The width of the shelf is  $200 \text{ km}$  and the linear slope then extends  $200 \text{ km}$  farther offshore. The storm center enters the coast at the alongshore position of  $2140 \text{ km}$ . This happens approximately 21 hours after the start of the simulation. It is immediately evident that 24 hours after the onset of the wind, water is piled up against the coast in the area where the low pressure center hits the coast. Shelf waves propagating with the coast to the right are also evident. The alongshore wavelengths of these waves are varying from somewhat less than  $1000 \text{ km}$  to approximately  $2400 \text{ km}$ . As a consequence of dispersion the longer waves propagate faster than the shorter ones and therefore a wave train with gradually shorter wavelengths will develop in the area. Using the computer code developed by Huthnance (Gordon and Huthnance 1987), Gjevik (1991) calculated the dispersion relation for the lowest mode *barotropic* shelf waves, corresponding to this slope/shelf bathymetry. A plot showing this dispersion relation is presented in Fig. 4. Note that the computation of this relation is based on inviscid linear theory. Gjevik argued that for the relative long waves considered, the effect of the rather weak stratification on the lower-order modes was likely to be small. From the dispersion curve for the lowest barotropic mode,

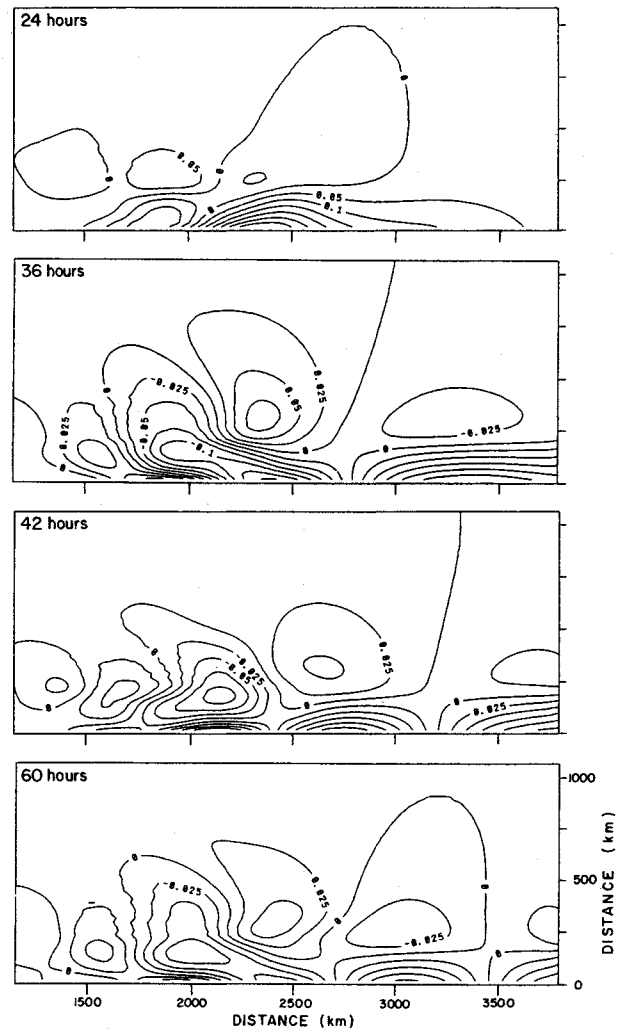


FIG. 3. Temporal evolution of surface elevation (m).

it is found that the longest waves, that is, waves with wavelengths longer than  $2000 \text{ km}$ , are practically non-dispersive, so that the phase speed is constant and equal to the group velocity. According to theory, the amplitude of these waves is characterized by a linear decay from the coast to the shelf break. As seen in Fig. 3, the amplitude of the wave propagating out to the right in the plots after 36 hours and 42 hours has this linear decay. From these plots a total wavelength of approximately  $2360 \text{ km}$  and a phase speed (or equivalently group velocity) of about  $20 \text{ m s}^{-1}$  can be estimated for this propagating shelf wave. This phase speed is in good agreement with that which is found from the analytic dispersion relation for the long waves of the lowest barotropic shelf wave mode.

For shorter waves the analytic dispersion relation shows that the group velocity of the lowest mode decreases and finally, for waves with a wavelength of  $837.8 \text{ km}$  and period of  $21.2 \text{ hours}$ , reaches a zero value. Since the group velocity represents the propagation

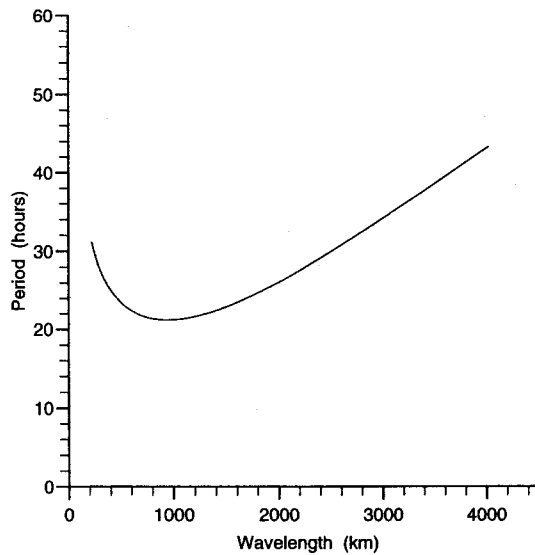


FIG. 4. Dispersion curve for the lowest barotropic shelf wave mode.

speed of the wave energy, this means that wave components with this wavelength will remain in the area where they were generated a long time after the storm has passed. In Fig. 5 the modal structure of the zero group velocity component, that is, the component with wavelength 837.8 km and period 21.2 h, is shown. [Figure 5 is taken from Gjevik (1991).] The maximum values for both surface elevation and current are found at the shelf break. Note, however, that as much as about 36% of the maximum sea level amplitude is retained 400 km offshore, at the border between the slope and the deep ocean. In the experiment discussed here such waves are clearly present in the shelf area near the storm track. This is for instance seen in Fig. 3, when comparing the pattern of the sea surface elevation in this area after 36 and 60 hours. Even though the amplitude is less after 60 hours (as a result of model friction), the surface contours are almost identical, indicating an oscillation with an approximate period of 24 hours. This long periodic oscillation is more easily revealed when looking at time series of the surface elevation. In Fig. 6, time series displaying the surface elevation during a period of 10 days are given for station 1 and 2. These long series were produced by an extended run of this experiment. The sites of these stations are depicted in Fig. 1. Station 1 is situated in the deeper part of the slope (330 km offshore), whereas station 2 is located at the shelf break (210 km offshore). The storm center passes almost directly over the location of station 1 (nearest approach 14 km) after 12 hours of simulation. The distance of nearest approach between the cyclone center and station 2 is about 100 km, that is, five grid distances. Figure 6 clearly confirms that oscillations with a period of about 22 hours persist at these stations throughout the 10 days of simulation. In agreement with inviscid linear theory (see Fig. 5), the amplitude

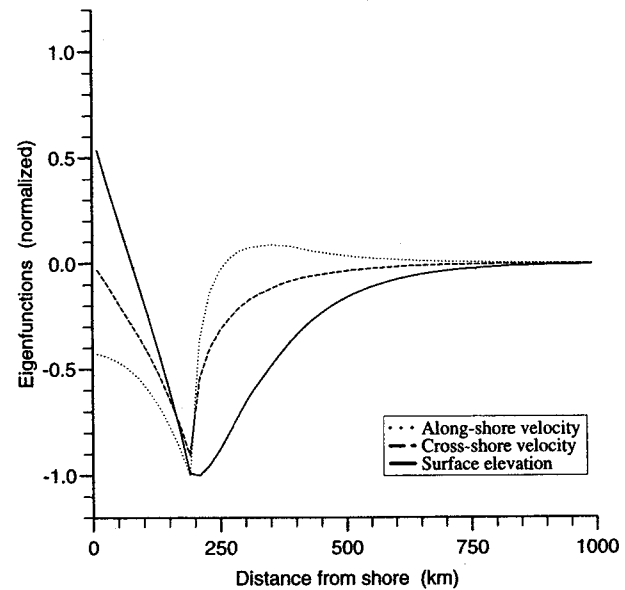


FIG. 5. Modal structure for surface elevation and the cross- and alongshore velocity components for the lowest barotropic shelf wave component with wavelength 837.8 km and period 21.2 h.

of these oscillations is largest at the shelf break, that is, at station 2.

In the upper part of the ocean, in the area directly forced by the wind stress, the response is strongly dominated by near-inertial oscillations. This is also to be expected from earlier studies of the ocean response to traveling storms (mostly studies of tropical hurricanes), for example, Price (1981), Cooper and Thompson

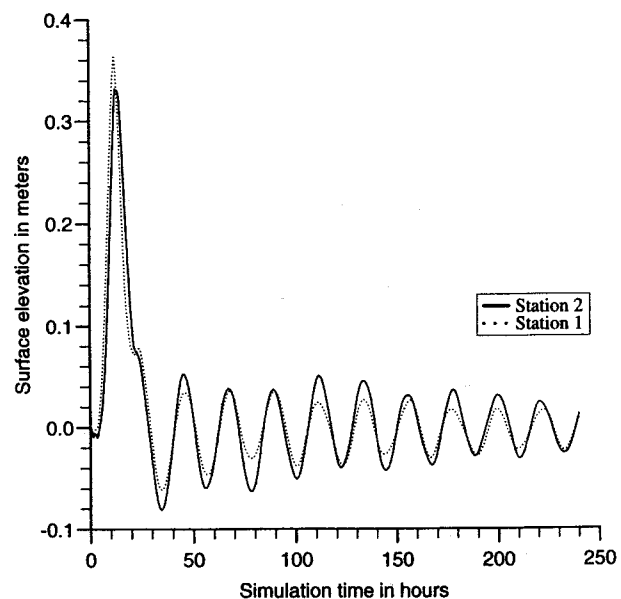


FIG. 6. Time series of surface elevation (10 days simulation) for stations on the slope (station 1) and at the shelf break (station 2).

(1989a,b), Shay et al. (1990), Gjevik (1991), among others. Except for Cooper and Thompson and Gjevik these authors have only considered oceans with a flat bottom.

In Fig. 7, time series of current (speed and direction) at depths of 10 and 100 m are shown for stations 1 and 3. Station 3 is located centrally on the shelf (110 km offshore). The storm center passes station 3 at a minimum distance of 170 km (8.5 grid distances) about 15 hours after the start of the simulation. In Fig. 7 the direction is given in degrees and zero degree is in the direction of the  $x$  axis in Fig. 1, the angle increasing as the vector rotates counterclockwise, that is, cyclonically.

At 10-m depth the current vector at both stations rotates clockwise with a period of about 13 hours, which is close to the calculated inertial period of 13.4 hours for this area. At station 1 the maximum speed is about  $0.9 \text{ m s}^{-1}$  after 18 hours and remains above  $0.5 \text{ m s}^{-1}$  for the rest of the simulation period (72 hours total simulation time). On the shelf, at station 3, the maximum speed is slightly lower ( $0.8 \text{ m s}^{-1}$  after 18 hours) and the speed is significantly lower thereafter.

At station 1 the near-inertial period is dominant even at the depth of 100 m. In the time series of current direction at this depth for station 3, however, there is

evidence of a lower frequency in addition to the near-inertial period. As discussed earlier in this section, it is natural to connect this slower oscillation with the barotropic shelf mode, with a period of about 22 hours. The speed at 100 m is significantly lower than at 10 m for both stations.

Plots of the simulated horizontal current field after 36 hours at 10, 100, and 1000 m below the surface are shown in Fig. 8. This is 6 hours after the storm was switched off. The velocity at 10 m, with amplitudes of  $0.7 \text{ m s}^{-1}$ , demonstrates the complex nature of the strong near-inertial oscillating current field that persists in the wake of the storm track. Based on the numerical results the horizontal wavelength of the wake pattern can be roughly estimated to about 800 km. Gill (1982) has shown that for storms moving with a speed large compared with the first baroclinic wave speed, the inertial oscillating wake will exhibit waves with horizontal wavelengths,  $\lambda$ , close to  $2\pi U/f$ , where  $U$  is the speed of the storm. Here  $U = 15 \text{ m s}^{-1}$ , which definitely is larger than the fastest baroclinic phase speed, and  $f = 1.3 \times 10^{-4} \text{ s}^{-1}$ , resulting in  $\lambda = 725 \text{ km}$ . This is rather close to our estimated result. The current pattern shown in the plot is also very similar to the mixed layer wake currents found by Cooper and Thompson (1989a,b).

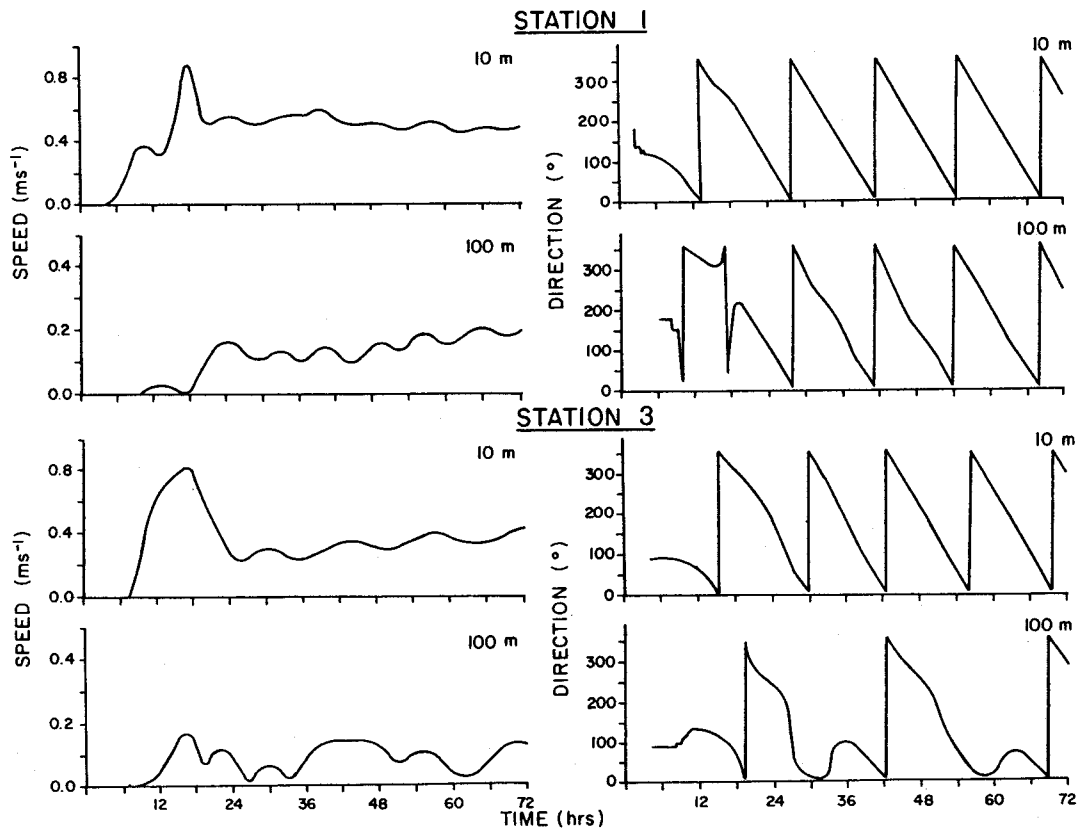


FIG. 7. Time series of current at depths 10 and 100 m for stations on the slope (station 1) and on the shelf (station 3).

